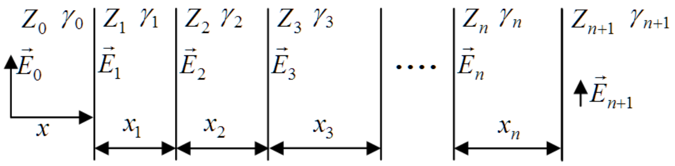

Fig. 5. Parameters of the multilayer structure: Z_i is the characteristic impedance; γ_i is the propagation constant; x_i is the thickness of *i*-th layer along the direction of wave propagation; E_i is the absolute value of the electric field vector in *i*-th layer

In accordance with the energy conservation law, the following equation is true for absolute values of the transmission T_{ij} and reflection R_{ij} coefficients:

$$\left|R_{ij}\right|^2 + \left|T_{ij}\right|^2 = 1. \tag{5}$$

For the given value of E_0 in the initial medium (air), one can obtain the value of E_1 at the boundary of layers with numbers 0 and 1 inside the layer of number 1: $E_1 = T_{01}E_0$. The amplitude of the electric field vector decreases due to the propagation in the layer of number 1, when the propagation constant γ_1 has a complex value (the layer of number 1 has certain conductivity or it is below cutoff waveguide). Taking into account the multiple reflections from the first and the second boundaries of the first layer, one can write for the amplitude E_2 in the layer of number 2 (at the second boundary) the following formula [19]:

$$E_2 = \frac{\exp(-i\gamma_1 x_1)T_{01}T_{12}}{1 - R_{01}R_{12}\exp(-2i\gamma_1 x_1)}E_0, \tag{6}$$

where the formula for the sum of decreasing geometric series with the geometric ratio $q = R_{01}R_{02}\exp(-2i\gamma_1 x_1)$ is used.

The following notations are introduced:

$$T_1 = \frac{\exp(-i\gamma_1 x_1)T_{01}T_{12}}{1 - R_{01}R_{12}\exp(-2i\gamma_1 x_1)},\ R_1 = \pm\sqrt{1 - T_1^{\ 2}}, \tag{7}$$

where T_1 and R_1 are the effective transmission and effective reflection coefficients corresponding to the layer of number 1.

By the use of notation (7), value of E_3 can be written in the form:

$$E_3 = \frac{\exp(-i\gamma_1 x_1)\exp(-i\gamma_2 x_2)T_{01}T_{12}T_{23}E_0}{(1 - R_{01}R_{12}\exp(-2i\gamma_1 x_1))(1 - R_1 R_{23}\exp(-2i\gamma_2 x_2))}, \tag{8}$$

or $E_3 = T_1 T_2 E_0$ where $T_2 = \dfrac{\exp(-i\gamma_2 x_2)T_{23}}{1 - R_1 R_{23}\exp(-2i\gamma_2 x_2)}$.

By iteration of the described steps, the following result for multilayer structure consisting of n layers is obtained:

$$E_{n+1} = E_0\prod_{i=1}^{n}T_i,\ T_1 = \frac{\exp(-i\gamma_1 x_1)T_{01}T_{12}}{1 - R_{01}R_{12}\exp(-2i\gamma_1 x_1)},$$
$$T_i = \frac{\exp(-i\gamma_i x_i)T_{ij}}{1 - R_{i-1}R_{ij}\exp(-2i\gamma_i x_i))},\ R_{i-1} = \sqrt{1 - \left(\prod_{k=1}^{i-1}T_k\right)^2},\ i > 1. \tag{9}$$

The result analogous to (9) can be written for the magnetic field component H of the electromagnetic wave when the incident plane wave in the initial medium is considered [22]. Proposed iterative method for the shielding effectiveness calculation of the multilayer structure based on formulas (9), formulas for the magnetic field component, and formulas (1) takes into account the contribution of all multiple reflected waves from all of boundaries between the layers. For cases, which are important in practice, each layer provides a sufficient attenuation of wave amplitude by the propagation. So, formulas (9) can be simplified since the contribution of the multiple reflected waves arising only in the nearest layer is considered for the field amplitude calculation at the boundary. The simplified formula for the shielding effectiveness of the multilayer structure takes the form:

$$S_{ml} = \sum_{i=1}^{n}S_i, \tag{10}$$

where S_i is the shielding effectiveness of the layer with number i calculated by the use of (7) with substitution of values $T_{i-1\ i}$, $R_{i-1\ i}$, $T_{i\ i+1}$, and $R_{i\ i+1}$ that are defined by (4) and (5) for the front and back boundaries of the layer.

IV. Worst-Case Estimation of Shielding Effetiveness of Gaskets

A. Model of Solid Metal Gasket

The choice of the worst-case model of the solid metal gasket in the form presented in Figure 2 is based on the following features of its application and mounting. Firstly, as for the size and surface finishing of the solid metal gasket, they must satisfy to the high quality class. The shape of the solid metal gasket must precisely correspond to the shape of placement location. In practice, to provide the tight joint of the metal gasket in placement location, the additional gasket made from rubber or plastic is used. Secondly, when the solid metal gasket is operated in corrosive environment, the insulating oxide film arises at its surface. Therefore, two narrow slots instead of the one wide slot are considered in framework of solid metal gasket model.

Method of combined wall [19] is used to calculate the shielding effectiveness in the framework of the developed model. This method is based on the calculation of electromagnetic wave energy penetrating inside the enclosure through the non-uniform wall consisting of regions. For the estimation of the shielding effectiveness of the illuminated wall, the following formula is used [19]:

$$S_{f(E,H)} = -10\lg\left(\sum_{i=1}^{N} 10^{-S_{i(E,H)}/10} A_i / A_0\right), \qquad (11)$$

where $S_{i(E,H)}$, is the shielding effectiveness of the region with the number i of the area A_i, $A_0 = A_1 + A_2 + ... + A_n$ is the total area of the combined wall.

When the slot in the illuminated wall does not contain the gasket (initial case), only two regions are considered: the slot of the length l and the width w and the enclosure wall with the thickness h, conductivity σ_1 and permeability μ_1.

When the model of the solid metal gasket is considered, the combined illuminated wall consists of the following regions: two narrow slots of the length l and the width Δw filled by dielectric of permittivity ε_2; the solid gasket of the thickness h made from the metal of conductivity σ_2 and permeability μ_2; the remaining area of the illuminated wall is the enclosure wall with parameters given above.

The model of below cutoff waveguide is used for description of the slots shielding effectiveness $S_{m(E,H)}$ (index m corresponds to the regions compared to the slots). The shielding effectiveness of the slot is calculated by the use of formulas (1) and (7) when the initial medium is air, and the final environment is the waveguide compared to the cavity inside the enclosure with propagation constant and characteristic impedance defined by (3). Propagation constant γ_s and characteristic impedance Z_s of the below cutoff waveguide associated to the slots are calculated by formula (3) by substitution the slot dimensions (l and w (or Δw)) and velocity $v = c/\sqrt{\varepsilon_2}$. The shielding effectiveness of the solid wall is calculated according to the model developed in [23].

The shielding effectiveness of the enclosure with the gasket in aperture is estimated on the basis of the deterministic and the worst-case models of the shielding effectiveness [19] for the observation points inside the enclosure. The worst-case model of the reverberation components AFC in the high-frequency band is defined by the line connecting amplitudes at resonance frequencies obtained in framework of the deterministic model. The intrinsic Q-factor of the enclosure is defined by the shielding effectiveness $S_{f(E,H)}$ and $S_{b(E,H)}$ of the front and back walls respectively.

The contribution of solid metal gasket to the shielding effectiveness calculation is defined by formula (2). The comparison of results obtained in framework of developed model and results of numerical simulation by FDTD and MOM methods is presented in Figure 6. Parameters of modeling are: $a = b = 0.3$ m; $c = 0.12$ m, $l = 0.1$ m, $h = w = 16$ mm; $\Delta w = 1$ mm. Enclosure wall material is aluminum. The material of the gasket is brass. Dielectric inside the slot is air.

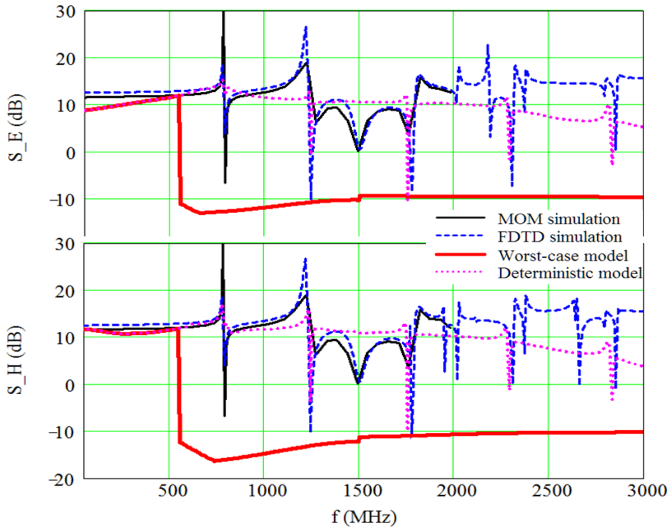

Fig. 6. AFC of the contribution (2) of the solid metal gasket to the shielding effectiveness. Coordinates of the observation point are (0, 150, 100) mm

As it is shown in the Figure 6, the use of the gasket in the form of solid metal does not decrease the field level at the frequencies corresponding to the cavity resonances. Since the enclosure intrinsic Q-factor depends on the shielding effectiveness of its walls, the more the shielding effectiveness the less energy flow penetrates through the walls and the more energy is accumulated inside the cavity. Therefore, the values of the field amplitude at resonances in the case of gasket presence can exceed the values in the case of the gasket absence when the enclosure has high Q-factor.

The influence of compression forces to the shielding effectiveness is negligible small for this type of gasket [14].

B. Model of Gasket in Form of Metal Spring Fingers

The model presented in Figure 3 contains a two-dimension periodic structure. For calculation the shielding effectiveness of such structure one can obtain the special form of formula (11). Let's consider a system consisting of two regions with the shielding effectiveness S_1 and S_2 of areas A_1 and A_2 respectively. The whole area of combined wall is A_0 and the incident flux density is p_0. The energy penetrating through the two regions of combined wall $p_1 A_1 + p_2 A_2$ defines the shielding effectiveness that calculated by formula:

$$S_{1\,(E,H)} = -10\lg\left(\frac{p_1 A_1 + p_2 (A_0 - A_1)}{p_0 A_0}\right), \qquad (12)$$

When the combined wall consists of N identical elements of area A_1 (for example, N identical apertures that are below cutoff waveguide), the formula of shielding effectiveness takes the form:

$$S_{N\,(E,H)} = -10\lg\left(\frac{N p_1 A_1 + p_2 (A_0 - N A_1)}{p_0 A_0}\right), \qquad (13)$$

Therefore, the correction used for accounting the number of apertures is as follows:

$$S_{N\,(E,H)} = -10\lg N - 10\lg\left(\frac{1+K_{12}\left(A_0/(NA_1)-1\right)}{1+K_{12}\left(A_0/A_1-1\right)}\right), \quad (14)$$

where $K_{12} = p_2 / p_1 = 10^{0.1\cdot(S_1-S_2)}$.

The structure under consideration (Figure 3) consists of the solid metallic wall and the periodical structure. The first region of periodic structure is the rectangular aperture (described by below cutoff waveguide) and the second region is multilayer, which consist of two thick metallic walls (front and back) and cylindrical waveguide (cutoff frequency is $f_{cc} = c\eta_{11}/(2\pi\cdot r\sqrt{\varepsilon_2})$, $\eta_{11} = 1.8412$).

The additional to (14) correction factor is introduced for the periodic structure calculation. This factor is described by the summand $K_3 = 20\lg(\tanh(P/8.69))$, $P = \exp(-i\gamma_s h)$ [24], where P characterizes the attenuation by propagation in aperture considered as below cutoff waveguide.

Calculation of the shielding effectiveness is performed by the use of formulas (9), (14) and (11) for the given set of the gasket parameters: $n = \Delta n = 5$ mm, $r = 7.5$ mm, $t = 0.5$ mm, (gasket is made from brass). Initial parameters of the enclosure and the slot are the same as in previous case (see subsection IV.A). Comparison of the results obtained in framework of the developed model with results of simulation by FDTD and MOM [25] methods is presented in Figure 7.

The effect of the shielding effectiveness increasing near the resonant frequency $f_{cc} = 11.72$ GHz of the cylindrical waveguide compared to rings noted in [26] is not analyzed because the maximum modeling frequency is 3 GHz.

The shielding effectiveness of the gasket in form of metal spring fingers increases with the increase of the compression forces because the slot width and ring radius are decreased.

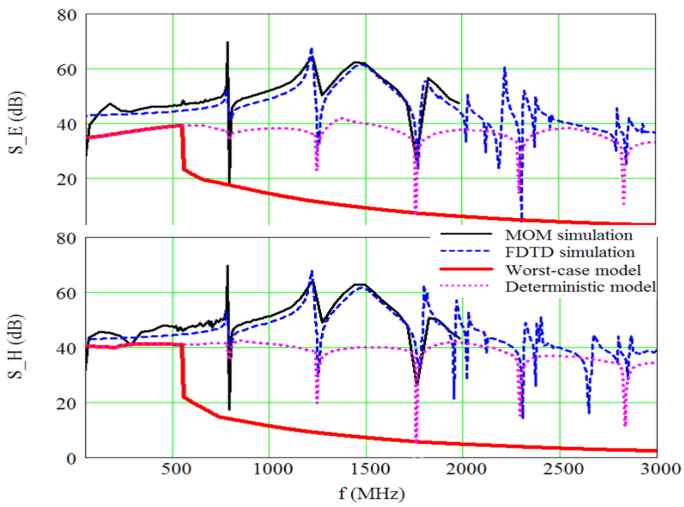

Fig. 7. AFC of the contribution (2) of gasket in the form of metall spring fingers to the shielding effectiveness. Coordinates of the observation point are (0, 150, 100) mm

C. Model of Gasket in Form of Wire Mesh

The model of the shielding effectiveness of the gasket in the form of wire mesh (see Figure 4) is based on the consideration of the multilayer structure (section III) and the model of combined wall. The shielding effectiveness is calculated in accordance with the technique proposed in [24] for each layer in the form of the wire mesh. It should be noted that the use of this technique provides the same results as the use of model based on formula (14) with the additional correction factor K_3. In the case of wire mesh, when the width of metallic partitions between apertures is small relative to the aperture dimension ($A_0/(NA_1)-1 \approx 0$), formula (14) takes the form:

$$S_{N\,(E,H)} = -10\lg N + 10\lg\left(1+K_{12}(N-1)\right), \quad (15)$$

The first shielding layer (Figure 4) is a wire mesh and the next layer is the waveguide compared to the slot in the illuminated wall. This three-dimensional periodical structure is repeated along Oy axis (see Figure 1). Since the layer in the form of the wire mesh has the sufficient shielding effectiveness, simplified formula (10) can be used for calculation of the multilayer structure shielding effectiveness. The initial medium is free space and the final environment is a waveguide compared to the cavity inside the enclosure.

Validation of the model for this gasket type is carried out for the following set of parameters. The wire mesh is made from the brass, the wire depth $d = 0.4$ mm; the mesh cell (length of the aperture) $\Delta d = 0.36$ mm; the number of layers in form of the mesh is 5; the distance between layers $\Delta h = 0.36$ mm. Parameters of enclosure with the slot are the same as in previous cases. Comparison of results obtained in framework of the model with results on numerical simulation by FDTD and MOM [25] methods is presented in Figure 8.

The presence of the compression forces leads the increasing of the shielding effectiveness for this gasket type.

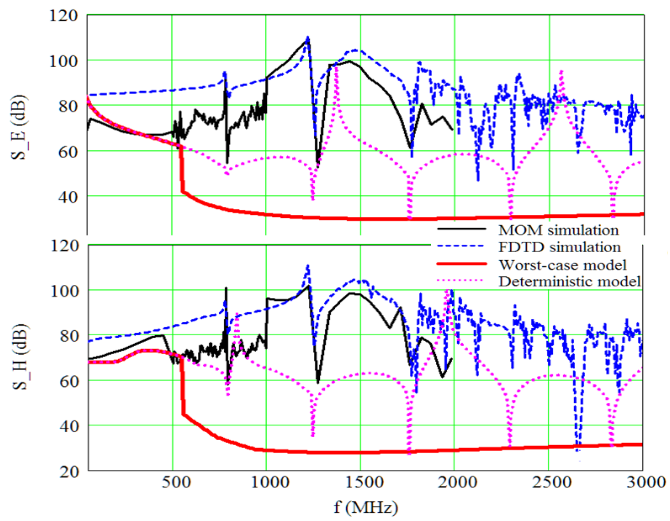

Fig. 8. AFC of the contribution (2) of gasket in the form of the wire mesh to the shielding effectiveness. Coordinates of the observation point are (0, 150, 100) mm

V. CONCLUSION

In this paper, the wideband computationally-effective worst-case model of electromagnetic field shielding by a metallic enclosure is developed for the cases when apertures in the enclosure walls are covered by gaskets. The model can be applied for estimation of intensity of the electric and magnetic components of the field inside a vehicle or ship compartment which can be approximated by rectangular waveguide and has the high Q-factor.

Models for three types of EMI gaskets are considered. Gaskets in form of stamped or formed metal plates are used when stationary joint between system body elements must be provided. Gaskets in the form of metal spring fingers and knitted wire mesh can be used as for stationary mounting as well as for sealing of slots subjected to dynamic forces, for example, slots around the edges of doors and hatches.

Comparison of the results obtained in the framework of the developed model with the results of numerical simulation shows the sufficient accuracy (about 10 dB in low-frequency band) of the model for cases of the solid metal gasket and the gasket in form of metal spring fingers.

Further development of the model can be associated with consideration of the energy absorption inside the compartments in order to introduce realistic value of Q-factor. The analysis of other gasket types, including gaskets that provide the increase in the shielding effectiveness by energy absorption, is an actual problem, too.

References

[1] Tong X.C., Advanced materials and design for electromagnetic interference shielding, CRC Press Taylor and Francis Group, An Informa business, NY, 2009, 324 p.

[2] Christopoulos C. Principles and Techniques of Electromagnetic Compatibility. Raton, FL: CRC Press, 1995.

[3] Gooch J.W., Daher J.K., Electromagnetic shielding and corrosion protection for aerospace vehicles. Springer Scieence+Busines Media, LLC, NY, 2007, 127 p.

[4] Paul C.R., Introduction to Electromagnetic Compatibility, 2nd ed., Wiley, Hoboken, NJ, 2006, 983 p.

[5] Catrysse J., et al. The Importance of continuous and homogeneous Gasket Conductivity up to 40 GHz// Proc. of Int. Symp. on EMC "EMC Europe 2013", Brugge, Belgium, Sept. 2-6, 2013, pp. 536-540.

[6] MIL-STD-464C. Electromagnetic Environmental Effects Requirements for Systems. U.S. Government Printing, Washington, 2010.

[7] IEC 61000-4-21 International Standard. Elecromagnetic Compability (EMC) – Part 4-12. Testing and measurement techniques – Reverberation chamber test methods. Edition 2.0, 2011-01

[8] IEEE Std 299-2006, IEEE Standard Method for Measuring the Effectiveness of Electromagnetic Shielding Enclosures, IEEE Electromagnetic Compatibility Society, IEEE, 3 Park Avenue, New York, NY 10016-5997, USA, 28 February 2007

[9] Gifuni A., A Proposal to Improve the Standard on the Shielding Effectiveness Measurements of Materials and Gaskets in a Reverberation Chamber, // IEEE Trans. on EMC Vol. 59 No. 2, 2017, pp. 394-403.

[10] Marvin A.C., at al. A Proposed New Definition and Measurement of the Shielding Effect of Equipment Enclosures // IEEE Trans. on EMC Vol. 47 No. 3, 2005, pp. 589-601.

[11] Catrysse J., et al. A new stripline measuring setup for the characterisation of conductive gaskets up to 18 GHz// Proc. of the IEEE Int. Conf. on EMC, F. Lauterdale, Florida, USA, July 2010, pp. 165-170.

[12] Faraji P., et al. SE Measurements with a TEM Cell to Study Gasket Reliability// Proc. of the IEEE Int. Conf. on EMC, USA, August, 2013, pp. 462-465.

[13] Pouhe D., Tcheg P. Study on Corrosion-Induced Shielding-Degradation of EMI Gaskets// IEEE Trans. on EMC Vol. 58 No. 4, 2016, pp. 1052-1059.

[14] Kuncel G., Mechanical force considerations in the use of emi-environmental gaskets// Proc. of the IEEE Int. Conf. on EMC, USA, Oct., 1980, pp. 1-6.

[15] Davidson D.B., Computational electromagnetics for RF and microwave engineering, 2-nd ed, Cambridge University Press, 2011.

[16] Goergakopoulos S.V., Britcher C.R., Balanis C.A. HIRF Penetration Through Apertures: FDTD Versus Measuremants// IEEE Trans. on EMC, Vol 43, No. 3, 2001, pp. 282-294

[17] Robinson M.P., et al. Analytical Formulation for the Shielding Effectiveness of Enclosures with Apertures// IEEE Trans. on EMC, Vol. 40, No. 3, Aug. 1998, pp. 240-248.

[18] Collin R.E., "Field Theoty of Guided Waves", IEEE Press, New York, 1990, 852 p.

[19] Tsyanenka D., Sinkevich E.; Arlou Y., Wideband Worst-Case Model of Electromagnetic Field Shielding by Metallic Enclosure with Apertures// Proc. of Int. Symp. on EMC "EMC EUROPE 2017", Angers, France, September 4-8, 2017, pp. 1-6.

[20] Tsionenko D., et al. Computationally-Effective Ultra-Wideband Worst-Case Model of Electromagnetic Wave Diffraction by Aperture in Conducting Screen// Proc. of Int. Symp. on EMC "EMC Europe 2014", Gothenburg, Sweden, Sept. 1-4, 2014, pp.1287-1292.

[21] Grigor'ev A.D., Electrodynamics and microwave ingeneering, Moscow, Higher Scool, 1990, 335 p. (In Russian).

[22] Klinkenbusch L., On the Shielding Effectiveness of Enclosures// IEEE Trans. on EMC, Vol. 47, No. 3, Aug. 2005, pp. 589-601.

[23] Cowdell R.B. Simplified shielding // IEEE Int. Symp. on EMC, 1967, pp. 399-412.

[24] Jarva W. Shielding efficiency calculation methods for screening, waveguide ventilation panels, and other perforated electromagnetic shields // Proc 7th Conf. on RIR and EMC, 1961, pp. 478-498.

[25] EMCoS Ltd., EMCoS EMC Studio, www.emcos.com, 2018

[26] Yoneda S., et al. A GHz-band Gasket-Free Electromagnetic Shielding Structure with Built-in Cascaded SIW Resonators// Proc. of Int. Symp. on EMC "EMC Europe 2014",Gothenburg, Sweden, Sept. 1-4, 2014, pp.432-437.